Coupling in concentric double quantum rings

A. Mühle, W. Wegscheider, and R. J. Haug

Citation: Appl. Phys. Lett. **91**, 133116 (2007); doi: 10.1063/1.2790828
View online: https://doi.org/10.1063/1.2790828
View Table of Contents: http://aip.scitation.org/toc/apl/91/13
Published by the American Institute of Physics

Coupling in concentric double quantum rings

A. Mühle[a)]
Institut für Festkörperphysik, Leibniz Universität Hannover, Appelstraße 2, 30167 Hannover, Germany

W. Wegscheider
Angewandte und Experimentelle Physik, Universität Regensburg, Universitätsstraße 31, 93040 Regensburg, Germany

R. J. Haug
Institut für Festkörperphysik, Leibniz Universität Hannover, Appelstraße 2, 30167 Hannover, Germany

(Received 13 July 2007; accepted 9 September 2007; published online 28 September 2007)

We designed a device consisting of two concentric quantum rings in a GaAs/AlGaAs heterostructure. The outer ring is connected to leads while the inner ring is only capacitively coupled to the rest of the system. Measuring electronic transport in a regime with strong coupling to the leads we found that the conductivity not only shows an Aharonov-Bohm effect with a periodicity fitting to the diameter of the outer ring but also another component matching the inner ring. This can be explained by magnetic-field dependent charge redistributions in the inner ring which affect the outer ring via Coulomb interaction. © *2007 American Institute of Physics*. [DOI: 10.1063/1.2790828]

Semiconductor quantum rings have proven to be an inherently interesting field of study because of their multiple connected geometry. They can be used as phase-sensitive quantum interferometers. A typical example is the single-particle Aharonov-Bohm effect[1] that can be directly observed in the transport spectrum when the device is coherently traversed by electrons and pierced by a magnetic flux.[2–4] In the recent literature an Aharonov-Bohm effect has also been proposed for rings in which two independently injected electrons enclose a magnetic flux by their combined paths,[5] but this is not visible directly in the conductance and had to be verified indirectly.[6] Here we present the modulation of the electronic transport through a ring by Aharonov-Bohm oscillations arising in a second one with both rings interacting only electrostatically.

Our device consists of two concentric quantum rings directly written into a two-dimensional electron gas (2DEG) and connected to lateral leads using the technique of local anodic oxidation.[7] So far concentric double rings have only been reported to be produced by self-organized growth,[8,9] which leaves them unsuitable for the direct study of lateral transport properties. But on our structure lateral transport measurements through the outer ring not only show the expected Aharonov-Bohm effect with a period fitting to this ring's geometry but also an additional oscillation with a period matching the diameter of the inner ring. We attribute the latter to Coulomb coupling between both rings, which is schematically depicted in Fig. 1. We fabricated our device from a GaAs/AlGaAs heterostructure consisting of a 5 nm thick GaAs cap layer, 6.5 nm of AlGaAs, 2 nm AlAs, 2 nm GaAs, a Si-δ layer, a 18.5 nm wide AlGaAs barrier, and 1000 nm of GaAs (from top to bottom). The 2DEG is located 34 nm below the surface with an electron density of $n_e = 3.85 \times 10^{15}$ m^{-2} and a mobility of $\mu_e = 64.3$ m^2 V^{-1} s^{-1}. The inset in Fig. 2 shows an atomic force microscope image of the structure which was formed by local anodic oxidation. The 120 nm broad oxide lines separate two conducting ring-shaped areas from each other and from the two in-plane gates G1 and G2. The outer ring (ring I) is connected to the leads source (S) and drain (D) via two 100 nm wide point contacts, while the inner ring (ring II) is totally insulated from the rest of the structure. The point contacts can be tuned by G1 and G2. Ring II has an oxide dot with a diameter of 150 nm in its center. The ring's outer edge has a diameter of about 460 nm with a small ellipticity. The edges of ring I also show a small deviation from the circular shape. Its inner edge has an average diameter of 710 nm and its outer edge one of 1100 nm. The transport measurements presented in this work were performed with the sample mounted in a dilution refrigerator at the base temperature $T = 20$ mK. To adjust the effective width of the point contacts and therewith the coupling of ring I to the leads, voltages V_{G1} and V_{G2} could be applied individually to the respective gates G1 and G2. Without an externally applied voltage, the point contacts were closed, forming thin barriers. Only Coulomb-blockade peaks were visible in the transport when the voltages were swept close to this value but the Aharonov-Bohm effect was not observable in this regime. $V_{G1,G2}$ had to be set to positive values to reach a more open regime necessary for our observations. For the results shown here, it was stepped over the range from 370 to 440 mV and the same voltage $V_{G1,G2}$ was applied on both gates. Since ring II forms a totally insulated island (at small bias, the oxide barriers have resistances of several gigaohms), it only interacts capacitively with the rest of the device. Figure 1 depicts a schematic of this situation. An external magnetic field B was applied perpendicular to the

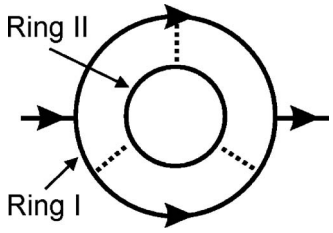

FIG. 1. A schematic of the electronic paths in the device. While the outer ring I is coupled to leads, the inner ring II forms an insulated island. Both rings couple capacitively, symbolized by the dotted lines.

[a)]Electronic mail: amuehle@nano.uni-hannover.de

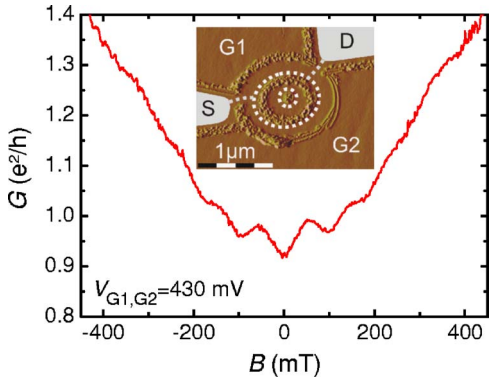

FIG. 2. (Color online) Conductance G as a function of B with $V_{G1,G2}$ =440 mV. Inset: Image of the device taken with an atomic force microscope. The dotted lines mark the Coulomb-coupled electronic paths around areas of 0.517 μm^2 (in ring I) and 0.046 μm^2 (in ring II) matching the observed Aharonov-Bohm frequencies.

plane of the rings. For each of the aforementioned gate configurations it was swept from −500 to 500 mT while the conductance G through ring I was investigated using standard lock-in technique. We restricted the magnetic field to this range because above 450 mT Shubnikov–de Haas oscillations become dominant, thereby obscuring the Aharonov-Bohm features. Figure 2 shows a typical measurement that was done at a gate voltage of 430 mV. The conductance of ring I rises from 0.9 to $1.6e^2/h$ with increasing magnetic field. A dip at zero field and superimposed weak oscillations are visible over the depicted range. Above a magnetic field of 350 mT, the onset of Shubnikov–de Haas oscillations is visible. To take a better look at the weak oscillations, every original curve was smoothed by boxcar averaging to yield the background which was then subtracted from the raw data, leaving only the oscillatory part of the signal. Comparison of the resulting curves reveals that the oscillations are independent from the voltage applied to the gates for the whole voltage range observed here. Resulting curves for three different gate voltages are shown in Fig. 3 where dotted lines mark the positions of some of the peaks. The oscillations have a peak-to-peak amplitude of $2.5\times10^{-2}e^2/h$ and a period over the magnetic field of ΔB=89 mT. A closer look at the curves reveals that another type of much weaker and higher frequent oscillations is also present in the signal. These small oscillations with an amplitude of up to

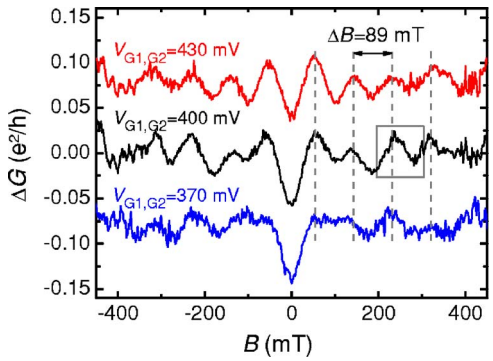

FIG. 3. (Color online) Difference ΔG between the conductance G and the nonoscillating background as a function of B for three values of $V_{G1,G2}$. The curves are offset for clarity. A gate-independent oscillation with a period of 89 mT is clearly visible. The box marks the range of the data shown in Fig. 4.

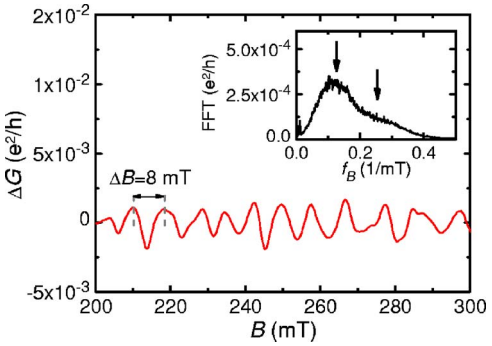

FIG. 4. (Color online) Small Aharonov-Bohm oscillations of ring I over B in the conductance after subtraction of the lower frequency components and averaging over 370 mV$\leq V_{G1,G2}\leq$440 mV showing a period of 8 mT. Inset: FFT of the same data resulting in a large peak at ~1/8 mT^{-1} and a smaller feature at the double frequency (both marked by arrows).

$3.5\times10^{-3}e^2/h$ are more easily visible when the lower frequencies are removed from the data. Therefore the curves were smoothed again to acquire a background that was then subtracted from the data. Furthermore, the results for all used gate voltages were averaged to suppress the random noise and improve the clarity of the features. A part of the extracted small oscillations is presented in Fig. 4 over the magnetic field interval that is marked by a box in Fig. 3. The small oscillations have a period of ΔB=8 mT. This is also confirmed by the fast Fourier transformation (FFT) of the signal as shown in the inset of the figure, where peaks (marked by arrows) can be seen at the according frequency of 0.125 mT^{-1} as well as at the double frequency of 0.250 mT^{-1}.

Looking at the correlation between an Aharonov-Bohm period ΔB and the corresponding area A enclosed by the electrons given by

$$A = \frac{h}{e\Delta B}, \tag{1}$$

where h is Planck's constant and e is the elementary charge, shows that the small oscillations' period fits to an area of 0.515 μm^2. A circle of this size is surrounded by a path with a diameter of 810 nm which thus is located in the inner region of the outer ring. The small oscillations can therefore be attributed to the normal Aharonov-Bohm effect for electrons traversing ring I. The location of the path is marked in the inset in Fig. 2 by the dotted curve that is connected to the source and drain areas. Comparison of the small oscillations' amplitude to the background yields a visibility of less than half a percent. Such a small value for the expected Aharonov-Bohm effect in ring I can be explained by the assumption of imperfections in the actual shape of the confinement potential. This has been reported to drastically reduce or even suppress the Aharonov-Bohm amplitude in quantum rings.[10] When examining the other set of features in the transport through ring I, i.e., the large oscillations as seen in Fig. 3, the application of Eq. (1) shows that an Aharonov-Bohm effect with a period of 89 mT corresponds to an enclosed area of 0.046 μm^2 with an accordant diameter of 243 nm. Thus the surrounding path lies inside of ring II surrounding the oxide dot. In the inset in Fig. 2 the dotted circle around the center marks this location. This result is somehow astonishing, since no current is flowing through ring II,

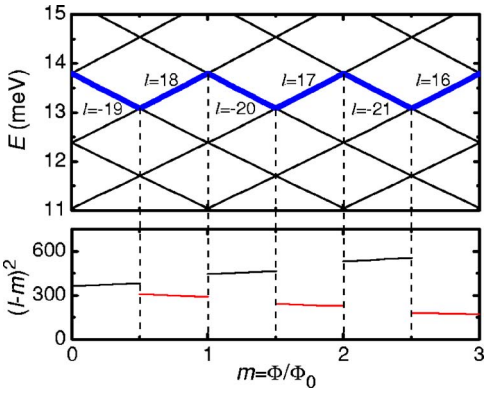

FIG. 5. (Color online) Upper part: Theoretical energy spectrum of ring II over the number m of enclosed flux quanta. The bold line marks the levels at the Fermi edge. Lower part: Evolution of the term $(l-m)^2$ important for the radial extension of the electronic wave function over the same axis.

which is just Coulomb coupled to ring I where the current is flowing.

Most of the theoretical work about concentric quantum rings found in the literature does not describe a comparable system, since the focus lies on tunnel-coupled systems.[11,12] One model of separated concentric rings suggests that Coulomb drag slightly alters the Aharonov-Bohm oscillations,[13] but does not describe the transfer of the Aharonov-Bohm period from one ring to the other. Thus we start the analysis of the experimental results by comparing our ring II to an ideal, closed ring with an energy spectrum, as shown in Fig. 5. There the electronic levels in the ring take the form of shifted parabolas as they are plotted over the magnetic flux Φ piercing through its center. If Φ is given as the number m of enclosed flux quanta Φ_0, the energies of the states are described by

$$E_{m,l} = \frac{\hbar^2}{2m^* r_0^2}(m+l)^2. \tag{2}$$

Here l is the angular momentum quantum number, $\hbar$ is the reduced Planck constant, m^* is the effective mass of an electron, and r_0 is the radius of the ring which is assumed to be one dimensional in this model. With increasing magnetic flux, the electrons change the state which they occupy and thereby also the angular momentum quantum number l due to level crossings. Since we calculate a Fermi energy of 13.76 meV from the carrier density of the 2DEG, the electrons at the Fermi edge inside the ring follow the zigzag line marked in the upper part of Fig. 5. Starting with zero flux the level occupied has $l=19$, while for higher fields the angular momentum quantum number develops successively as $l=18$, -20, 17, -21, 16, and so on. Looking only at values for parts of the zigzag line with the same slope shows that the absolute value of l increases by 1 from one falling segment to the next $(|l|=19,\ldots,20,\ldots,21,\ldots)$ while it decreases by 1 from one rising segment to the next $(|l|=\ldots,18,\ldots,17,\ldots,16,\ldots)$. Thus the angular momentum quantum number alternates between two sets of values whereas its absolute value steadily gets larger in the one and continuously drops in the other. To investigate the spatial distribution of the electrons on ring II one has to use a model which takes the two dimensionality of the ring into account. The model of Ref. 14 shows that the radial extension of the wave function is dependent on the term $(l-m)^2$. This term is dominated by the absolute value of l when m is small, as in our case where the observed range of magnetic field corresponds to only up to five flux quanta enclosed by ring II. Therefore the aforementioned alternating change of $|l|$ between two sets of values leads to a similarly alternating evolution of the whole term $(l-m)^2$, as depicted in the lower part of Fig. 5. In consequence, this should lead to a back and forth shift of the charge between distributions with wider and narrower radial extensions inside of ring II. Since the inner ring's Coulomb potential is not shielded from the outer ring, this redistribution of its charge leads to a modulation of the confinement potential of ring I which then is mirrored in the observed large oscillations in the conductance G. An alternative approach to explain charge redistributions inside of ring II lies in the assumption of a magnetic-field dependent polarization. This could arise from charge being periodically moved in or out of a trap due to the influence of the enclosed flux on the electrons' wave function. Similar shifts of charge distributions in rings without rotational invariance are described in Refs. 15–17. Obviously, for an exact description of the situation inside of our device further theoretical work would be necessary.

In conclusion, electronic transport through the outer ring of a concentric double quantum ring device was examined in dependence of a perpendicular magnetic field B. The observed oscillations show two distinct components with different frequencies. One of them is caused by the Aharonov-Bohm effect in the directly measured ring while the other one is attributed to the influence of the inner ring, whose electrons are spatially redistributed with its own Aharonov-Bohm period. This influences the outer ring's confinement potential due to Coulomb coupling and accordingly causes an analog variation in the measured transport.

We acknowledge financial support by BMBF via nanoQUIT.

[1] Y. Aharonov and D. Bohm, Phys. Rev. **115**, 485 (1959).
[2] K. Ismail, S. Washburn, and K. Y. Lee, Appl. Phys. Lett. **59**, 1998 (1991).
[3] A. Fuhrer, S. Lüscher, T. Ihn, T. Heinzel, K. Ensslin, W. Wegscheider, and M. Bichler, Nature (London) **413**, 822 (2001).
[4] U. F. Keyser, C. Fühner, S. Borck, R. J. Haug, M. Bichler, G. Abstreiter, and W. Wegscheider, Phys. Rev. Lett. **90**, 196601 (2003).
[5] P. Samuelsson, E. Sukhorukov, and M. Büttiker, Phys. Rev. Lett. **92**, 026805 (2004).
[6] I. Neder, N. Ofek, Y. Chung, M. Heiblum, D. Mahalu, and V. Umansky, Nature (London) **448**, 333 (2007).
[7] M. Ishii and K. Matsumoto, Jpn. J. Appl. Phys., Part 1 **34**, 1329 (1995).
[8] T. Mano, T. Kuroda, S. Sanguinetti, T. Ochiai, T. Tateno, J. Kim, T. Noda, M. Kawabe, K. Sakoda, G. Kido, and N. Koguchi, Nano Lett. **5**, 425 (2005).
[9] T. Kuroda, T. Mano, T. Ochiai, S. Sanguinetti, K. Sakoda, G. Kido, and N. Koguchi, Phys. Rev. B **72**, 205301 (2005).
[10] V. A. Tkachenko, Z. D. Kvon, D. V. Sheglov, A. V. Latyshev, A. I. Toropov, O. A. Tkachenko, D. G. Baksheyev, and A. L. Aseev, JETP Lett. **79**, 136 (2004).
[11] P. Gartner and A. Aldea, Z. Phys. B: Condens. Matter **99**, 367 (1996).
[12] B. Szafran and F. M. Peeters, Phys. Rev. B **72**, 155316 (2005).
[13] T. V. Shahbazyan and S. E. Ulloa, Phys. Rev. B **55**, 13702 (1997).
[14] W.-C. Tan and J. C. Inkson, Semicond. Sci. Technol. **11**, 1635 (1996).
[15] M. Büttiker, Phys. Scr., T **T54**, 104 (1994).
[16] M. Büttiker, Nuovo Cimento Soc. Ital. Fis., B **B110**, 509 (1995).
[17] M. Büttiker and C. A. Stafford, Phys. Rev. Lett. **76**, 495 (1996).